



# Identification of reaction intermediates in AlCl<sub>3</sub>-mediated cyclocondensation reactions by simultaneous in situ ATR-FTIR and UV–vis spectroscopy



Sebastian Reimann<sup>a,b</sup>, Leif R. Knöpke<sup>b</sup>, Anke Spannenberg<sup>b</sup>, Angelika Brückner<sup>b</sup>, Oliver Kühn<sup>c</sup>, Peter Langer<sup>a,b,\*</sup>, Ursula Bentrup<sup>b,\*</sup>

<sup>a</sup>Leibniz-Institut für Katalyse e.V. an der Universität Rostock (LIKAT), Albert Einstein Str. 29a, 18059 Rostock, Germany

<sup>b</sup>Institut für Chemie, Universität Rostock, Albert-Einstein-Str. 3a, 18059 Rostock, Germany

<sup>c</sup>Institut für Physik, Universität Rostock, Wismarsche Str. 43–45, 18057 Rostock, Germany

## ARTICLE INFO

### Article history:

Received 25 October 2012

Received in revised form 9 January 2013

Accepted 16 January 2013

Available online 26 February 2013

### Keywords:

Cyclization

Lewis acids

IR spectroscopy

UV–vis spectroscopy

Reaction mechanisms

## ABSTRACT

Functionalized trifluoromethyl-substituted salicylates have been synthesized based on AlCl<sub>3</sub>-mediated cyclocondensation reactions using 4,4-dimethoxy-1,1,1-trifluorobut-3-en-2-one and 1,3-bis(silyloxy)-1,3-butadienes. Simultaneous in situ ATR-FTIR/UV–vis spectroscopic measurements were carried out for mechanistic studies. Real-time in situ spectroscopic investigations reveal the formation of an aluminum trichloride bidentate-butenone adduct as intermediate. The observed band shifts in the respective UV–vis spectra in consequence of complex formation could be explained by theoretical calculations. Lewis acidic solids (Al<sub>2</sub>O<sub>3</sub> and TiO<sub>2</sub>) were also successfully utilized. Due to the strong substrate adsorption on the solids detected by UV–vis-DRS and FTIR transmission spectroscopy the obtained yields were rather modest.

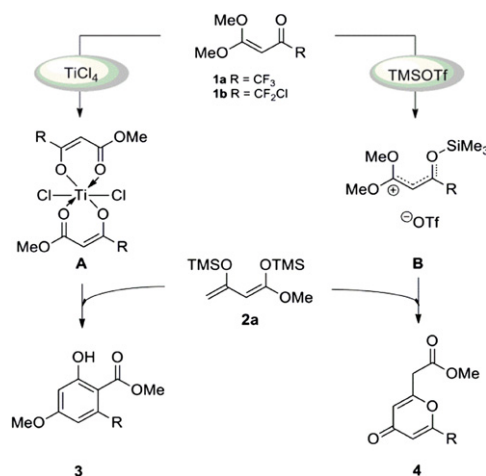
© 2013 Elsevier Ltd. All rights reserved.

## 1. Introduction

Lewis acid mediated formal [3+3] cyclocondensation reactions of 1,3-bis(silyloxy)-1,3-butadienes (Chan's dienes) with 1,3-dielectrophiles such as 3-alkoxy-2-en-1-ones, 1,3-ketoacetals, 1,3-keto-S,O-acetals or 3-silyloxy-2-en-1-ones represent an important method, which allows the one-pot synthesis of a great variety of six-membered carbocycles, which are not readily available by other methods.<sup>1,2</sup> This includes, for example, the synthesis of various functionalized salicylates, pyran-4-ones, phenols, and cyclohexenones being important as core structures to many biologically active small molecules.<sup>3</sup>

During the last years we intensively studied the scope of cyclocondensation reactions of 1,3-bis(silyloxy)-1,3-butadienes with electrophilic building blocks and found that the type of the employed Lewis acid has an important influence on the product distribution.<sup>4</sup> In this context we recently reported mechanistic studies of TiCl<sub>4</sub> and TMSOTf (trimethylsilyl trifluoromethanesulfonate) mediated cyclization reactions of 1,3-bis(silyloxy)-1,3-butadiene **2a** with butenones **1a,b** (Scheme 1) showing that the

interaction of the Lewis acid with **1** played a decisive role in this process. On the one hand salicylates **3** were observed using TiCl<sub>4</sub> while on the other hand pyran-4-ones **4** were observed when



**Scheme 1.** General reaction scheme. Influence of TiCl<sub>4</sub> and TMSOTf on the product distribution in cyclocondensation reactions.

\* Corresponding authors. E-mail addresses: peter.langer@uni-rostock.de (P. Langer), ursula.bentrup@catalysis.de (U. Bentrup).

TMSOTf was employed. Results of ATR-FTIR and UV–vis spectroscopic studies revealed that TiCl<sub>4</sub> formed a bis-chelate complex **A** while TMSOTf interacts with only one site of **1**, forming an ionic species **B**.<sup>5</sup>

Against this background also other Lewis acids like AlCl<sub>3</sub> should be suitable to use in this kind of reaction having a high reactivity as well and showing a different product selectivity than observed for TiCl<sub>4</sub> or TMSOTf.<sup>6</sup> In this context, several examples have been reported for TiCl<sub>4</sub> or BF<sub>3</sub>·OEt<sub>2</sub> promoted cyclization reaction of Chan's diene with 1,3-dielectrophiles.<sup>7,8</sup> However, to the best of our knowledge cyclocondensation reactions and their mechanistic investigation using AlCl<sub>3</sub> as mediating reagent have not been reported to date.

Comparing TiCl<sub>4</sub> and AlCl<sub>3</sub>, the electronic properties should differ from each other. Thus, the spectroscopic detection (UV–vis) of different transition states formed by interaction with the substrates has to be assumed. However, AlCl<sub>3</sub> is known to form chelate complexes with bidentate ligands like acetyl acetone.<sup>9</sup> Therefore, a similar intermediate as described in our previous study with TiCl<sub>4</sub><sup>5</sup> should be expected if AlCl<sub>3</sub> interacts with **1**.

Herein, we report the first AlCl<sub>3</sub>-mediated formal [3+3] cyclocondensation reactions of 4,4-dimethoxy-1,1,1-trifluorobut-3-en-2-one **1a** and 1,3-bis(silyloxy)-1,3-butadienes **2** affording a variety of functionalized 4-methoxy-6-(trifluoromethyl) salicylates with yields up to 59%. The interaction of AlCl<sub>3</sub> with both reactants was studied by ATR-FTIR and UV–vis spectroscopy. While UV–vis spectroscopy gives insight about changes in the electronic state of the molecules, ATR-FTIR spectroscopy reveals information on the molecular changes in terms of vibrations of characteristic bonds. Simultaneously in situ ATR-FTIR/UV–vis spectroscopic measurements were applied to study the influence of the temperature during the cyclization reaction. In this way comprehensive information about the reaction system is available because the same sample is analyzed at the same time.

Furthermore, Al<sub>2</sub>O<sub>3</sub> and TiO<sub>2</sub> were used as mediating Lewis acids in the described reaction system because of their easier handling and separation after the reaction. Due to the strong adsorption behavior of the substrates the yields were rather modest. In this context UV–vis-DRS and FTIR spectroscopy in transmission mode were applied to analyze the adsorbed substrates.

## 2. Results and discussion

### 2.1. Synthetic studies

4,4-Dimethoxy-1,1,1-trifluorobut-3-en-2-one **1a** and 1,3-bis(silyloxy)-1,3-butadienes **2a–j** were prepared from the known literature procedures.<sup>4b,10</sup> The AlCl<sub>3</sub>-mediated reaction of **1a** with 1,3-bis(silyloxy)-1,3-butadienes **2a–j** afforded 4-methoxy-6-(trifluoromethyl)salicylates **3a–j** in 47–59% yield, respectively (Table 1, Scheme 2). The reaction conditions were thoroughly optimized for

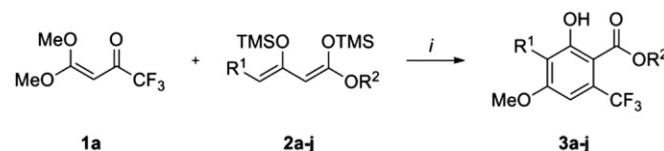
**Table 1**  
Synthesis of **3a–j**

<b>2, 3</b>	R <sup>1</sup>	R <sup>2</sup>	Yield of <b>3a–j</b> <sup>a</sup> [%]
a	H	Me	59 (47) <sup>b</sup>
b	H	<i>i</i> -Pr	58 (36) <sup>b</sup>
c	H	<i>i</i> -Bu	46
d	H	<i>n</i> -Bu	53
e	H	<i>i</i> -Pent	46
f	H	<i>n</i> -Oct	51
g	Me	Me	50 (34) <sup>b</sup>
h	Et	Me	58
i	<i>n</i> -Non	Me	52
j	<i>n</i> -Tetradec	Me	47

<sup>a</sup> Isolated yields.

<sup>b</sup> Reported yields in parantheses.<sup>4b</sup>

compound **3a** (Table 2), the structure of which was elucidated by 2D NMR spectroscopic methods (NOESY and COSY).



**Scheme 2.** Synthesis of **3a–j**. Reagents and conditions: (i) AlCl<sub>3</sub> (0 °C), CH<sub>2</sub>Cl<sub>2</sub>, –78 to 20 °C, 12–14 h.

**Table 2**  
Optimization of the synthesis of **3a**

Ratio of <b>1a/2a</b> [mmol]	AlCl <sub>3</sub> <sup>a</sup> [mmol]	CH <sub>2</sub> Cl <sub>2</sub> [mL]	Yield of <b>3a</b> <sup>b</sup> [%]
1:2	—	2	0
1:2	1 (25 °C)	2	49
1:2	2 (25 °C)	2	36
1:1	1 (0 °C)	2	28
1:2	1 (0 °C)	2	59
1:2	0.5 (0 °C)	2	26
1:2	2 (0 °C)	2	34
1:2	1 (0 °C)	5	51

<sup>a</sup> Addition of AlCl<sub>3</sub> at corresponding temperature.

<sup>b</sup> Isolated yields.

Applied concentration, temperature (addition of AlCl<sub>3</sub> and **2a**), and stoichiometry played important roles. The best yield could be obtained when the butenone **1a** was activated with AlCl<sub>3</sub> at 0 °C and the diene **2a** was added at –78 °C, when the reaction was carried out in a highly concentrated solution, and when an excess (2.0 equiv) of **2a** was employed. The reaction without AlCl<sub>3</sub> was unsuccessful. Products **3a–j**, containing the CF<sub>3</sub> group in *ortho* position to the ester group, were formed with excellent regio-selectivity. The formation of the other regioisomer, containing the CF<sub>3</sub> group located *para* to the ester group was not observed in these examples. This finding is consistent with the results made by Bunescu et al.<sup>4b</sup> who observed the same product- and regio-selectivity using TiCl<sub>4</sub> instead of AlCl<sub>3</sub>. However, the utilization of AlCl<sub>3</sub> could enhance the yields of **3** up to 22% (Table 1).

### 2.2. In situ studies: reaction monitoring by ATR-FTIR and UV–vis spectroscopy

According to the optimized synthesis protocol the butenone **1a** was activated with AlCl<sub>3</sub> at 0 °C while the diene **2a** was added after cooling at –78 °C. Then, the reaction mixture was warmed up to room temperature over a 12–14 h period. To investigate the activating effect and specific interaction of AlCl<sub>3</sub> with both reactants in dependence on temperature, simultaneous in situ ATR-FTIR/UV–vis spectroscopic measurements were exemplarily performed using **1a** and **2a** as substrates. For the in situ experiments the warm-up period of the reaction mixture was shortened to 4 h, which has been found to be adequate for getting comparable results as found by normal synthesis protocol.

The in situ ATR-FTIR spectra recorded during the reaction of **1a** with **2a** in the presence of AlCl<sub>3</sub> are displayed in Fig. 1. The first spectrum (Fig. 1a) shows **1a** dissolved in CH<sub>2</sub>Cl<sub>2</sub> at 20 °C. Important bands occur at 1683 cm<sup>–1</sup> with a shoulder at 1707 cm<sup>–1</sup>, which belong to the ν(C=O) vibration and at 1558 cm<sup>–1</sup>, which can be assigned to a ν(C=C) vibration. When AlCl<sub>3</sub> is added to **1a** at 0 °C followed by cooling the reaction mixture to –60 °C, the band of the ν(C=O) vibration is shifted to lower wavenumbers and appears at 1628 cm<sup>–1</sup> with increased intensity (Fig. 1b). This band shift indicates the interaction of **1a** with AlCl<sub>3</sub> via its carbonyl group. Pasykiewicz et al.<sup>11</sup> reported also a strong ν(C=O) band at 1628 cm<sup>–1</sup> for a monomeric aluminum methyl 2-hydroxybenzoate

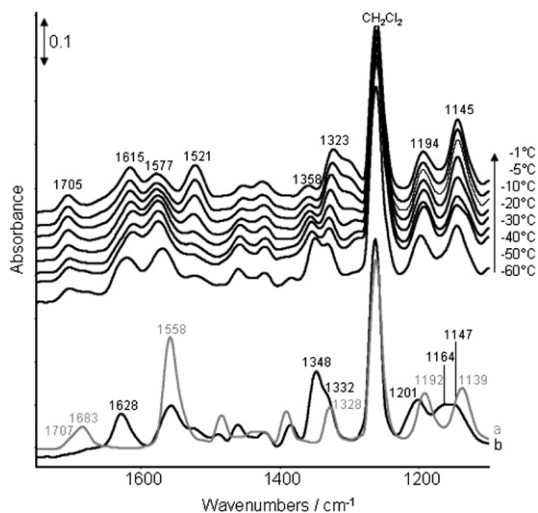


**Fig. 1.** In situ ATR-FTIR spectra of the  $\text{AlCl}_3$ -mediated reaction: (a) **1a** in  $\text{CH}_2\text{Cl}_2$  ( $c=0.5 \text{ mol L}^{-1}$ ) at  $20^\circ\text{C}$  without  $\text{AlCl}_3$ , (b) **1a**+ $\text{AlCl}_3$  at  $-60^\circ\text{C}$  in 1:1-mixture (molar ratio); and of **1a**+ $\text{AlCl}_3$ +**2a** as 1:1:2-mixture (molar ratio) at  $-60$ ,  $-50$ ,  $-40$ ,  $-30$ ,  $-20$ ,  $-10$ ,  $-5$ , and  $-1^\circ\text{C}$ .

chelate complex. Additional bands occur at  $1348$ ,  $1201$ ,  $1164$ , and  $1147 \text{ cm}^{-1}$ . While the bands at  $1348$ ,  $1201$ , and  $1147 \text{ cm}^{-1}$  result from shifted  $\nu(\text{C-F})$  and  $\nu(\text{C-O})$  modes of the methoxy and  $\text{CF}_3$  groups of **1a**, the band at  $1164 \text{ cm}^{-1}$  is related to  $\nu(\text{C-O-Al})$  vibration.<sup>11</sup> Simultaneously, the intensity of the  $\nu(\text{C=C})$  band is decreased, which was also observed when **1a** forms a bis-chelate complex with  $\text{TiCl}_4$ .<sup>5</sup>

The in situ ATR-FTIR spectra of the reaction mixture after dosing the diene **2a** to the 1:1-mixture of **1a** and  $\text{AlCl}_3$  at  $-60^\circ\text{C}$  are shown in Fig. 1 as well. Starting from spectrum b in Fig. 1 the most significant changes during the warming period from  $-60^\circ\text{C}$  to  $-1^\circ\text{C}$  resulted in the appearance of new bands in the region of the  $\nu(\text{C=O})$ ,  $\nu(\text{C=C})$ ,  $\nu(\text{C-F})$ , and  $\nu(\text{C-O})$  vibrations at  $1705$ ,  $1615/1577/1521$ ,  $1358/1323$ , and  $1194/1145 \text{ cm}^{-1}$ , respectively. These changes reflect the formation of an intermediate complex, which cannot be assigned in detail based on the existing data. For further elucidation additional ex situ investigations have been carried out (cf. Chapter 2.3). However, the positions of the characteristic bands occurring during reaction indicate that the reaction pathway is comparable to the  $\text{TiCl}_4$ -mediated reaction as described in our previous work.<sup>5</sup> A comparison of the characteristic bands observed in  $\text{AlCl}_3$ - and in  $\text{TiCl}_4$ -mediated reactions is shown in Table 3. The simultaneously recorded in situ UV–vis transmission spectra are displayed in Fig. 2.

**Table 3**  
Positions and assignments of bands observed during reaction

<b>1a</b> + $\text{AlCl}_3$ + <b>2a</b> ( $\nu/\text{cm}^{-1}$ )	<b>1a</b> + $\text{TiCl}_4$ + <b>2a</b> ( $\nu/\text{cm}^{-1}$ ) <sup>5</sup>	Assignment
1705	1706	$\nu(\text{C=O})$
1615	1616	$\nu(\text{C=C})$
1577	1581	$\nu(\text{C=C})$
1521	1521	$\nu(\text{C=C})$
1358/1323	1354/1306	$\nu(\text{C-F})$
1194/1145	1194/1143	$\nu(\text{C-O})/\nu(\text{C-O-M})$ (M=Al, Ti)

Due to the relatively high concentration the UV–vis spectra have an unusual shape. The spectrum of **1a** (Fig. 2a) shows at  $20^\circ\text{C}$  a broad band with maximum at  $335 \text{ nm}$  and a weak one at  $380 \text{ nm}$ , which might represent  $\pi \rightarrow \pi^*$  and  $n \rightarrow \pi^*$  transitions, respectively.

After the addition of  $\text{AlCl}_3$  at  $0^\circ\text{C}$  both signals are shifted to shorter wavelengths. The band positions are shifted further with decreasing temperature and finally appear at  $319 \text{ nm}$  and  $361 \text{ nm}$  at  $-60^\circ\text{C}$  (Fig. 2b), which might be caused by a stronger interaction

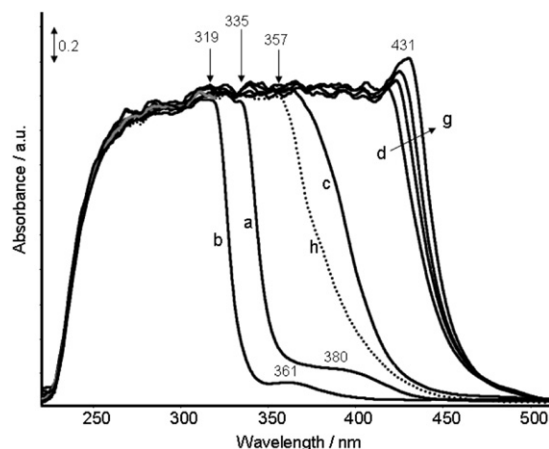


**Fig. 2.** In situ UV–vis transmission spectra of the  $\text{AlCl}_3$ -mediated conversion of **1a** and **2a** to **3a**: (a) 1 equiv **1a** in  $\text{CH}_2\text{Cl}_2$  ( $c=0.5 \text{ mol L}^{-1}$ ) at  $20^\circ\text{C}$ , (b) after addition of 1 equiv  $\text{AlCl}_3$  at  $-60^\circ\text{C}$ , (c)–(g) mixture of **1a**+ $\text{AlCl}_3$ +**2a** (molar ratio 1:1:2) at (c)  $-60^\circ\text{C}$ , (d) 20 min  $-60^\circ\text{C}$ , (e)  $-40^\circ\text{C}$ , (f)  $-30^\circ\text{C}$ , (g)  $-20^\circ\text{C}$ , and (h) after quenching with  $\text{HCl}$  (aq).

between **1a** and  $\text{AlCl}_3$ . The same effect was observed in the in situ ATR-FTIR experiment indicating the favored complex formation at lower temperatures within a continuous process.

The addition of **2a** at  $-60^\circ\text{C}$  provokes immediately a strong shift of the broad band to higher wavelengths (Fig. 2c), which is almost completed after 20 min (Fig. 2d). With increasing temperature the maximum is further shifted and reaches its maximum with  $431 \text{ nm}$  (Fig. 2e–g). Finally, the quenching with hydrochloric acid (aq) provokes a shift of the maximum to  $357 \text{ nm}$  (Fig. 2h).

The shift to lower wavelengths after mixing **1a** with  $\text{AlCl}_3$  is surprising because it is contrary to the observations with  $\text{TiCl}_4$ . In the  $\text{TiCl}_4$  route a strong shift to higher wavelengths could be observed when **1a** was mixed with  $\text{TiCl}_4$  due to the formation of a bis-chelate complex. The Ti-atom is bonded to the oxygen of the carbonyl group as well as to the oxygen atom of one methoxy group. Due to the delocalization of  $\pi$ -electrons an additional chromophore was created, which caused the shift of the absorption band to higher wavelengths in the UV–vis spectrum of the formed chelate complex. Hence, the shift to lower wavelengths in the UV–vis spectrum of the mixture of **1a** and  $\text{AlCl}_3$  indicates a different electronic state of the formed species.

For a better assignment of the bands occurring in the UV–vis spectra of **1a** and in the 1:1-mixture of **1a** with  $\text{AlCl}_3$ , diluted solutions have also been measured (Fig. 3).

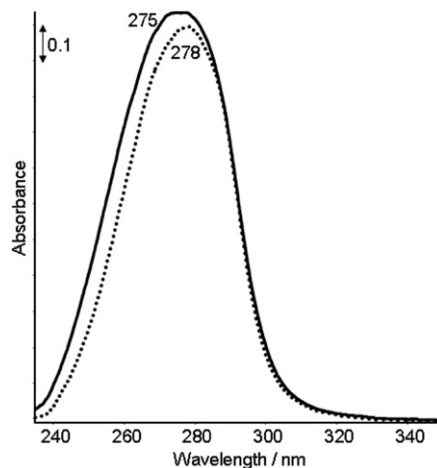


**Fig. 3.** Ex situ UV–vis spectra of **1a** in  $\text{CH}_2\text{Cl}_2$  (dotted line) and **1a**+ $\text{AlCl}_3$  in  $\text{CH}_2\text{Cl}_2$  (solid line) ( $c=5 \times 10^{-4} \text{ mol L}^{-1}$ ).

The spectrum of **1a** shows one discrete band with a maximum at 278 nm while the 1:1-mixture of **1a** and AlCl<sub>3</sub> (CH<sub>2</sub>Cl<sub>2</sub>,  $c=5 \cdot 10^{-4}$  mol L<sup>-1</sup>) shows a slightly more intense band at 275 nm. It is not clear if this difference indicates a significant change in the electronic structure or an interaction between **1a** and AlCl<sub>3</sub>. On the other hand, a band, which is characteristic for AlCl<sub>3</sub> and would occur at 240 nm<sup>12</sup> cannot be observed. Hence, an interaction between **1a** and AlCl<sub>3</sub> is likely.

One possible explanation for the shape of the UV–vis spectrum of the 1:1-mixture of **1a** and AlCl<sub>3</sub> might be the absence of d $\pi$ -electrons in the AlCl<sub>3</sub>-complex. Holm and Cotton<sup>13</sup> as well as Nakamoto et al.<sup>14,15</sup> pointed out that d $\pi$ –d $\pi$  and d $\pi$ –p $\pi$  interactions are important factors in the bond formation between metal and donor system. These interactions lead to bonds with resonance structures, which are also known as metalaromaticity.<sup>16</sup> For example, the Al–O bond in Al(acac)<sub>3</sub> is characterized as strongly covalent bond.<sup>14</sup> The missing d $\pi$ -electrons cause that less resonance structures appear and all bonds remain localized. Nakamoto et al.<sup>14,15</sup> described such complexes where the electrons remain localized in the ligand skeleton of the chelate ring as ‘weak complexes’. In contrast, the  $\pi$ -electrons and the d-electrons of the metal atom in strong chelate complexes tend to be more or less delocalized in the whole chelate ring. Consequently, the electronic structure is less changed in weak chelate complex, and the UV–vis spectrum of the mixture of **1a** and AlCl<sub>3</sub> shows no significant difference at room temperature. Furthermore, the interaction is obviously not strong enough to form a second chromophore as shown for the 1:1-mixture of **1b** and TiCl<sub>4</sub> in CH<sub>2</sub>Cl<sub>2</sub>.<sup>5</sup> Otherwise a second band or a shoulder should be observed.

### 2.3. On the nature of the intermediate complex of butenone **1a** with AlCl<sub>3</sub>

Summarizing the spectroscopic findings described above a specific interaction of **1a** with AlCl<sub>3</sub> could be detected. However, these findings do not allow to propose the structure of the formed intermediate complex.

For this reason it was tried to crystallize this complex from a 1:1-mixture of the butenone **1a** with AlCl<sub>3</sub> in CH<sub>2</sub>Cl<sub>2</sub> by slow evaporation and cooling. Single crystals were isolated and studied by X-ray structure analysis. The obtained molecular structure shows that an aluminum chelate complex **5** has been formed under the release of CH<sub>3</sub>Cl (Fig. S1, Table S1). The aluminum atom is surrounded by three butenone moieties leading to a distorted octahedral coordination with oxygen, which is reached by the coordination of two oxygen atoms of each chelate ligand (bond lengths and angles are discussed in Supplementary data). This finding is in contrast to the observed formation of a bis-chelate complex between TiCl<sub>4</sub> and **1a** as important reaction intermediate,<sup>5</sup> in which two chlorine atoms remain at the titanium atom as ligand (Fig. 4).

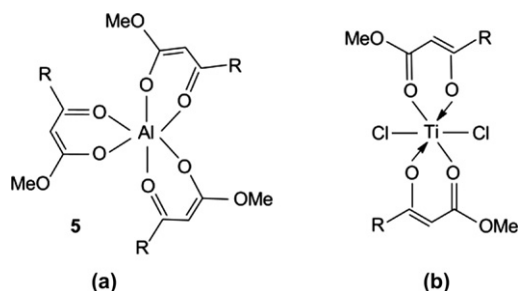


Fig. 4. Structures of the aluminum tris-chelate complex **5** formed between AlCl<sub>3</sub> and **1a** (a) and the bis-chelate complex formed between TiCl<sub>4</sub> and **1a** (b), according to the results of X-ray crystal structure analysis.

Starting from the molecular structure of the aluminum tris-chelate complex **5** (Fig. 4a) we calculated the excitation spectra in order to explain the shape of the UV–vis spectrum of the 1:1-mixture of **1a** and AlCl<sub>3</sub> theoretically (cf. Fig. 3). Therefore we used the time-dependent density functional theory employing the B3LYP functional (m3 grid) with a def2-TVZP basis set as implemented in Turbomole.<sup>17</sup> Likewise, the excitation spectra of the titanium bis-chelate complex (Fig. 4b) were investigated in comparison, too.

In the aluminum tris-chelate complex **5** the range between 197 and 285 nm was covered by the lowest 20 transitions. Here, a peak at 246 nm, whose orbital decomposition is given in Table S2 in Supplementary data, dominates the spectrum (Fig. S2). The spectrum of complex **5** is shifted about 14 nm to lower wavelengths in comparison to the spectrum of butenone **1a** possessing the dominant contribution at 260 nm. These results confirm our conclusion from the UV–vis spectra with regard to the electronic situation in the complex formed between **1a** and AlCl<sub>3</sub> (Fig. 3). In fact, inspecting the participating orbitals of the aluminum tris-chelate complex **5** in Fig. S3 one notices that the transitions are of intra-ligand  $\pi \rightarrow \pi^*$  type. The molecular orbitals of the aluminum-center are not involved due to the missing d $\pi$ -electrons causing a less resonated structure.

On the contrary, the electrons of the titanium bis-chelate complex are delocalized. The  $\pi$ -orbitals of the ligands are located in the manifold of the metal d-orbitals such that the lowest transitions are of  $\pi$  to d character (ligand-to-metal charge transfer type). Insofar, the different observed band shifts in the UV–vis spectra in consequence of complex formation of **1a** with TiCl<sub>4</sub> and AlCl<sub>3</sub>, respectively, could be explained by the theoretical calculations and confirm the description of the electronic state made by Nakamoto et al.<sup>14,15</sup>

Comparing the structures of both chelate complexes (Fig. 4) it can be expected that the aluminum tris-chelate complex **5** should be more stable than the chlorine-containing titanium bis-chelate complex. Thus, the question arises if the isolated complex **5** is really an intermediate complex in the reaction of **1a** with **2a**.

Inspecting the low frequency areas of the ATR-FTIR spectra of AlCl<sub>3</sub> mixtures with **1a** and **2a**, respectively, significant bands can be observed (Fig. 5).

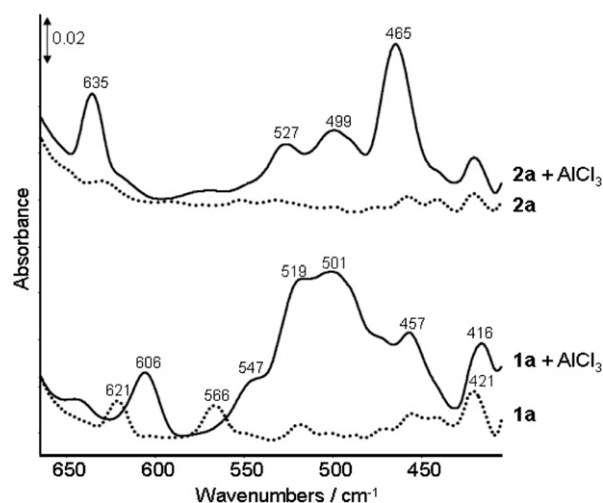


Fig. 5. Ex situ ATR-FTIR spectra of **1a** at 20 °C, **1a**+AlCl<sub>3</sub> at –50 °C, **2a** at 20 °C, and **2a**+AlCl<sub>3</sub> at 20 °C in CH<sub>2</sub>Cl<sub>2</sub> ( $c=0.5$  mol L<sup>-1</sup>).

The spectrum of **1a** shows only bands at 621, 566, and 421 cm<sup>-1</sup>, while no significant bands are observable in the spectrum of **2a** between 650 and 425 cm<sup>-1</sup>. In the spectrum of the mixture of **1a** with AlCl<sub>3</sub> the bands at 621, 566, and 421 cm<sup>-1</sup> are shifted to lower

wavenumbers (606, 547, and 416  $\text{cm}^{-1}$ ). Strong new bands can be seen at 519/501  $\text{cm}^{-1}$  and 457  $\text{cm}^{-1}$ , which are obviously caused by complex formation. Mixing of **2a** with  $\text{AlCl}_3$  provokes the appearance of new bands at 635, 527, 499, and 465  $\text{cm}^{-1}$ . A solution of  $\text{AlCl}_3$  in  $\text{CH}_2\text{Cl}_2$  with the same concentration was also measured for comparison (spectrum not shown). The observed bands at 622 and 441  $\text{cm}^{-1}$  can be assigned to the  $\nu_8$  and  $\nu_{13}$  vibration mode of  $\text{Al}_2\text{Cl}_6$ .<sup>18</sup> Such bands do not appear in the spectra of the  $\text{AlCl}_3$  mixtures with **1a** and **2a**.

Despite different intensities the new bands occurring in the spectra of both mixtures (Fig. 5) appear at comparable positions. Thus, the type of interaction in terms of substrate activation should be similar, which was found in the mixtures of **1a** and **2a** with  $\text{TiCl}_4$ , too.<sup>5</sup>

According to Weidlein et al.<sup>19</sup> the band of  $\nu(\text{Al}-\text{Cl})$  mode in methylmethoxyaluminumchloride  $\text{CH}_3(\text{OCH}_3)\text{AlCl}$  appears at 509/495  $\text{cm}^{-1}$ . Derouault et al.<sup>20</sup> investigated  $\text{AlCl}_3 \cdot \text{THF}$  complexes and reported bands at 525  $\text{cm}^{-1}$  and 439  $\text{cm}^{-1}$  belonging to  $\nu(\text{Al}-\text{Cl})$  and  $\nu(\text{Al}-\text{O})$  modes, respectively. Consequently, the observed bands of the  $\text{AlCl}_3$  complexes with **1a** and **2a** at 519/501  $\text{cm}^{-1}$  and 527/499  $\text{cm}^{-1}$  (Fig. 5) can be assigned to  $\nu(\text{Al}-\text{Cl})$  modes, while the bands at 457 and 465  $\text{cm}^{-1}$  result from  $\nu(\text{Al}-\text{O})$  vibrations.

In Fig. 6 the ATR-FTIR spectra of the crystallized aluminum tris-chelate complex **5** and the intermediate complex formed by interaction of **1a** with  $\text{AlCl}_3$  in  $\text{CH}_2\text{Cl}_2$  are compared. It is clearly seen that the  $\nu(\text{Al}-\text{Cl})$  bands at 519/501  $\text{cm}^{-1}$  do not appear, as expected, in the spectrum of the aluminum tris-chelate complex **5** (Fig. 6a). Considering the hash marked bands of the butanone moiety the band at 452  $\text{cm}^{-1}$  can clearly be assigned to the  $\nu(\text{Al}-\text{O})$  mode. The  $\nu(\text{Al}-\text{O})$  band and the bands of the butanone moiety appear slightly shifted in the spectrum of the intermediate formed complex of **1a** with  $\text{AlCl}_3$ , too (Fig. 6b). Thus, it can be concluded that the intermediate complex has another composition and structure as the crystallized tris-chelate complex **5**. Furthermore, the appearance of strong  $\nu(\text{Al}-\text{Cl})$  vibrations in the ATR-FTIR spectrum of the intermediate complex formed during the reaction clearly indicates that this complex does not accord with the crystallized aluminum tris-chelate complex **5**.

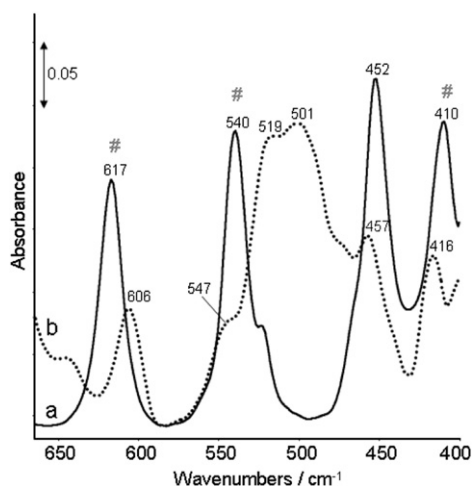
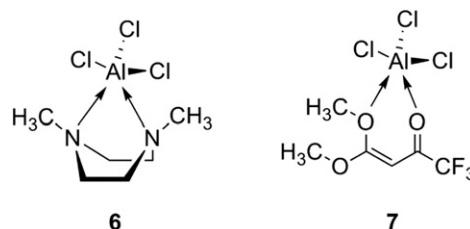


Fig. 6. ATR-FTIR spectra of the crystallized Al tris-chelate complex **5** (a) and the reaction intermediate of **1a**+ $\text{AlCl}_3$  (b) in  $\text{CH}_2\text{Cl}_2$  ( $c=0.5 \text{ mol L}^{-1}$ ) at 20 °C. The hash marked bands result from the butenone moiety.

It has to be considered, that the latter complex **5** is formed by a longtime crystallization process. Obviously, the chlorine-containing aluminum complex is the first intermediate formed by interaction of  $\text{AlCl}_3$  with **1a**, which is then slowly transformed by

losing chlorine. At the end a stable chlorine-free aluminum tris-chelate complex **5** is formed.

Based on the observed band positions in the ATR-FTIR spectrum alone it is difficult to propose the structure of the formed first intermediate complex. However, it should be mentioned in this context that Altwood et al.<sup>21</sup> reported the structural characterization of an aluminum trichloride-bidentate tertiary amine adduct **6** with trigonal bipyramidal coordination of the aluminum-center (Scheme 3). Unfortunately no FTIR or Raman spectroscopic data of this complex were given. Nevertheless, a similar structure **7** can be proposed for the observed intermediate complex formed between **1a** and  $\text{AlCl}_3$  (Scheme 3).



Scheme 3. Structure of the aluminum trichloride-bidentate tertiary amine adduct **6**<sup>21</sup> and postulated structure of the intermediate **7** formed between **1a** and  $\text{AlCl}_3$ .

#### 2.4. From single-phase to multi-phase systems: application of $\text{Al}_2\text{O}_3$ and $\text{TiO}_2$

The utilization of insoluble inorganic solids such as zeolites, titanium silicates, aluminas or silica gels in organic reactions is of considerable interest due to the easier catalyst separation, handling, process efficiency, and reduction of side-products.<sup>22</sup> Thus, we selected sulfate-free  $\text{TiO}_2$  and  $\text{Al}_2\text{O}_3$  as solid catalysts for elucidating their potential for this type of cyclocondensation reaction. The selection is based on the fact that the reaction works successfully in liquid phase with  $\text{TiCl}_4$  as well as  $\text{AlCl}_3$  and both solid acids possess Lewis acid centers. Furthermore, the adsorption of diketones on  $\text{TiO}_2$  nano-particles has been studied already with FTIR spectroscopy.<sup>23</sup> Additionally, alumina has been applied successfully in organic synthesis as versatile mediating acid such as intra- and intermolecular additions of OH groups, reductions, oxidations, substitutions, and decarboxylation reactions.<sup>24</sup>

The utilization of  $\text{Al}_2\text{O}_3$  in cyclocondensation reactions of **1a** with 1,3-bis(silyloxy)-1,3-butadienes **2a** and **2b** led to 4-methoxy-6-(trifluoromethyl)salicylates **3a** and **3b** in low yields (14–23%). No significantly improved yields were obtained by using  $\text{TiO}_2$  instead of  $\text{Al}_2\text{O}_3$  (Table 4). During the optimization it has been proved that  $\text{TiO}_2$  and  $\text{Al}_2\text{O}_3$  have to be activated under vacuum by repeated heating for 2–3 h. The reaction with non-activated  $\text{TiO}_2$

Table 4  
Synthesis of **3a,b** mediated by  $\text{Al}_2\text{O}_3$  and  $\text{TiO}_2$

2,3	R <sup>1</sup>	R <sup>2</sup>	$\text{CH}_2\text{Cl}_2$ [mL]	Mediating solid	Yield of <b>3a</b> [%]
a	H	OMe	3	$\text{Al}_2\text{O}_3$	14
a	H	OMe	1	$\text{Al}_2\text{O}_3$	17
a	H	OMe	0	$\text{Al}_2\text{O}_3$	0
b	H	Oi-Pr	1	$\text{Al}_2\text{O}_3$	23
a	H	OMe	1	$\text{TiO}_2$	13
b	H	Oi-Pr	1	$\text{TiO}_2$	15

<sup>a</sup> Isolated yields.

and  $\text{Al}_2\text{O}_3$  did not proceed. While Ranu et al.<sup>24b</sup> reported the solvent-free Mukaiyama–Michael addition of silyl-enol ethers to alkyl vinyl ketones on the surface of alumina, in our case a small amount of  $\text{CH}_2\text{Cl}_2$  seems to be important for the feasibility of the reaction.

Although the achieved yields were rather low, the utilization of  $\text{Al}_2\text{O}_3$  and  $\text{TiO}_2$  possessing Lewis acidity could be successfully accomplished. A possible reason for the comparable low yields might be the strong adsorption of substrates on the surface of the solids. Therefore, the interaction of **1a** and **2a** with  $\text{Al}_2\text{O}_3$  and  $\text{TiO}_2$  was studied by UV–vis–DRS and FTIR transmission spectroscopy.

Fig. 7 shows the UV–vis–DRS spectra of **1a** adsorbed on  $\text{Al}_2\text{O}_3$  and  $\text{TiO}_2$ . The spectra of pure  $\text{Al}_2\text{O}_3$  and  $\text{TiO}_2$  are included for comparison. The spectrum of pure  $\text{Al}_2\text{O}_3$  (Fig. 7a) shows two broad weak bands at 272 nm and 368 nm. Because  $\text{Al}_2\text{O}_3$  is known as UV–vis inactive, these bands result from impurities. The spectrum of **1a** adsorbed on  $\text{Al}_2\text{O}_3$  (Fig. 7b) shows one broad intense band at 274 nm indicating nicely the presence of adsorbed **1a**. The band position is comparable with that observed for pure **1a** and its 1:1-mixture with  $\text{AlCl}_3$  in  $\text{CH}_2\text{Cl}_2$  (cf. Fig. 3). The spectrum of the used pure  $\text{TiO}_2$  shows a characteristic broad band between 230 and 400 nm (Fig. 7c) the intensity of which is increased by adsorption of **1a** (Fig. 7d).

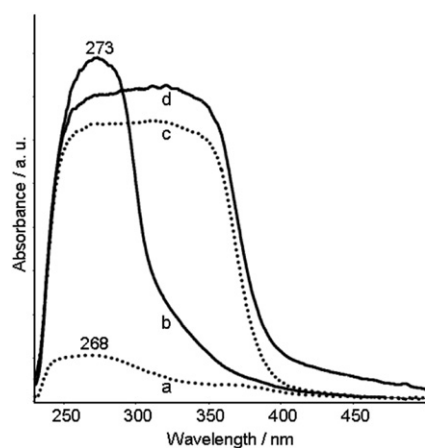


Fig. 7. UV–vis–DRS spectra of pure  $\text{Al}_2\text{O}_3$  (a), of **1a** adsorbed on  $\text{Al}_2\text{O}_3$  (b), of pure  $\text{TiO}_2$  (c), and of **1a** adsorbed on  $\text{TiO}_2$  (d).

Some more information concerning the nature of the adsorbates can be obtained from FTIR transmission spectra of self-supporting wafers of  $\text{Al}_2\text{O}_3$  on which the reactant **1a** or **2a** has been separately adsorbed (Fig. 8). Spectra of solutions of **1a** and **2a** in  $\text{CH}_2\text{Cl}_2$  and their mixtures with  $\text{AlCl}_3$  are included for comparison.

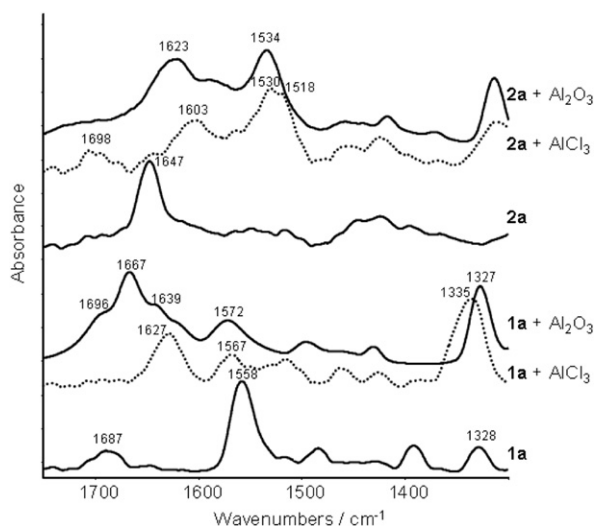


Fig. 8. ATR–FTIR spectra of **1a**, **2a** and their respective mixtures with  $\text{AlCl}_3$  in  $\text{CH}_2\text{Cl}_2$  ( $c=0.5 \text{ mol L}^{-1}$ ) and FTIR transmission spectra of **1a** and **2a** adsorbed on  $\text{Al}_2\text{O}_3$ .

The spectrum of **1a** adsorbed on  $\text{Al}_2\text{O}_3$  shows an intense band at  $1667 \text{ cm}^{-1}$  with shoulders at  $1696$ ,  $1639$ , and  $1629 \text{ cm}^{-1}$  being prominent for different  $\nu(\text{C}=\text{O})$  vibrations. The shift of the carbonyl band of **1a** to lower wavenumbers and splitting indicate an interaction of **1a** with the surface of  $\text{Al}_2\text{O}_3$ . Furthermore, the appearance of four different  $\nu(\text{C}=\text{O})$  points to the fact that **1a** adsorbs in a different manner. On the one hand the band at  $1667 \text{ cm}^{-1}$  with shoulder at  $1696 \text{ cm}^{-1}$  might be prominent for **1a** physisorbed on  $\text{Al}_2\text{O}_3$  due to the weak interaction with the surface of the  $\text{Al}_2\text{O}_3$ . On the other hand the bands at  $1639$  and  $1629 \text{ cm}^{-1}$  are caused by **1a** chemisorbed on  $\text{Al}_2\text{O}_3$ . Hence, the carbonyl group is strongly involved in the adsorption mechanism. As a result of this interaction the  $\nu(\text{C}=\text{C})$  band is shifted from  $1558$  to  $1572 \text{ cm}^{-1}$ , while the position of the  $\nu(\text{C}-\text{F})$  band at  $1328 \text{ cm}^{-1}$  remains unchanged.

The  $\nu(\text{C}=\text{C})$  band of **2a** at  $1647 \text{ cm}^{-1}$  shifts to lower wavenumbers if adsorbed on  $\text{Al}_2\text{O}_3$  while a new band appears at  $1534 \text{ cm}^{-1}$ , which cannot be surely assigned. Comparing the adsorbate spectra of **1a** and **2a** on  $\text{Al}_2\text{O}_3$  with those obtained from the respective mixtures of **1a** and **2a** with  $\text{AlCl}_3$  some similarities concerning characteristic band positions of  $\nu(\text{C}=\text{O})$  and  $\nu(\text{C}=\text{C})$  are obvious. This suggests that the interaction of **1a** and **2a** with  $\text{Al}_2\text{O}_3$  proceeds in a similar way as observed with  $\text{AlCl}_3$  in liquid phase.

### 3. Conclusions

Lewis acids like  $\text{AlCl}_3$ ,  $\text{Al}_2\text{O}_3$ , and  $\text{TiO}_2$  were successfully applied in cyclocondensation reactions using 1,3-bis(silyloxy)-1,3-butadienes and 4,4-dimethoxy-1,1,1-trifluorobut-3-en-2-one. The obtained products are trifluoromethyl-substituted salicylates possessing the same regio-selectivity as observed for  $\text{TiCl}_4$ -mediated cyclocondensation reactions.

The  $\text{AlCl}_3$ -mediated reaction proceeds via a comparable mechanism as found for  $\text{TiCl}_4$ . Differences were observed in the mode of activation of the reactants **1a** and **2a** with  $\text{AlCl}_3$ . The determined molecular structure of the crystallized intermediate complex formed by interaction of **1a** with  $\text{AlCl}_3$  indicates the formation of a chlorine-free aluminum tris-chelate complex. In contrast, in situ ATR–FTIR spectroscopic results revealed the appearance of strong  $\nu(\text{Al}-\text{Cl})$  vibrations in the spectrum of the intermediate complex formed during the interaction of **1a** and  $\text{AlCl}_3$  indicating the formation of a chlorine-containing complex. It is assumed that the long crystallization process leads to a transformation of the first formed chlorine-containing complex by losing chlorine.

Otherwise this finding nicely demonstrates the benefit of in situ spectroscopic studies enabling the real-time detection of intermediates formed in the respective reaction. In analogy to a published structure of an aluminum trichloride-bidentate tertiary amine adduct a similar aluminum trichloride bidentate-butenone adduct with trigonal bipyramidal coordination of the aluminum-center was proposed as possible structure of the formed intermediate complex.

Solid Lewis acidic  $\text{Al}_2\text{O}_3$  and  $\text{TiO}_2$  have also been applied in the cyclocondensation reaction. Due to the strong adsorption of the reactants on the solids, which was detected by UV–vis–DRS and FTIR transmission spectroscopy, the yields were rather modest. Obviously, the strong adsorption of the substrates hinders their effective interaction with each other.

## 4. Experimental section

### 4.1. General comments

All glassware used were heated and dried for several times under vacuum. All reactions were carried out under an inert atmosphere.  $\text{AlCl}_3$  was purchased from ACROS Organics (99.995%),  $\text{TiO}_2$  was received from Sachtleben Chemie GmbH, and  $\text{Al}_2\text{O}_3$  from

Sasol Germany GmbH. These solids were dried under vacuum by repeated heating for 2–3 h before use. The solvent (CH<sub>2</sub>Cl<sub>2</sub>, 99.8% extra anhydrous over molecular sieves, stabilized) was obtained from ACROS Organics. 1,3-Bis(silyloxy)-1,3-butadienes (**2**) were prepared according to a literature procedure from the corresponding  $\beta$ -ketoesters in two steps and used within a few days.<sup>10</sup> 4,4-Dimethoxy-1,1,1-trifluorobut-3-en-2-one (**1a**) was synthesized according to the protocol of Bunescu et al.<sup>4b</sup>

Thin layer chromatography (TLC) was run on Merck precoated aluminum plates (Si 60 F<sub>254</sub>). Column chromatography was performed using Merck Silicagel 60 (0.043–0.06 mm). NMR data were recorded on a Bruker ARX 300 and Bruker ARX 400 spectrometers. <sup>13</sup>C and <sup>1</sup>H NMR spectra were referenced to signals of CDCl<sub>3</sub>, respectively. Gas chromatography–mass analysis was carried out on an Agilent HP-5890 instrument with an Agilent HP-5973 Mass Selective Detector (EI) and HP-5 capillary column using helium carrier gas. ESI HRMS measurements were performed on an Agilent 1969A TOF mass-spectrometer. Elemental analysis was performed on a C/H/N/S-Microanalyser TruSpec CHNS (Leco).

## 4.2. General procedure for the synthesis of 3a–j

To a CH<sub>2</sub>Cl<sub>2</sub> solution (2.0 mL/1.0 mmol of **1a**) of **1a** (1.0 mmol) was added AlCl<sub>3</sub> (1.0 mmol) at 0 °C. The reaction mixture was cooled down to –78 °C and 1,3-bis(silyloxy)-1,3-butadienes **2** (2.0 mmol) was added. The reaction mixture was allowed to warm to 20 °C for 12 h with stirring. HCl was added to the solution (10%, 15.0 mL), and the organic and aqueous layers were separated. The latter was extracted with CH<sub>2</sub>Cl<sub>2</sub> (3 × 15.0 mL). The combined organic layers were dried (Na<sub>2</sub>SO<sub>4</sub>), filtered, and the filtrate was concentrated in vacuo. The residue was purified by flash chromatography using *n*-heptane and ethyl acetate.

## 4.3. Characterization data of 3a–j

**4.3.1. Methyl 2-hydroxy-4-methoxy-6-(trifluoromethyl)benzoate (3a).** Data have been previously reported.<sup>4b</sup> Starting with **1a** (0.184 g, 1.0 mmol), AlCl<sub>3</sub> (0.133 g, 1.0 mmol), **2a** (0.521 g, 2.0 mmol) in CH<sub>2</sub>Cl<sub>2</sub> (2.0 mL), **3a** was isolated as a yellowish solid (0.147 g, 59%); mp=64–66 °C. <sup>1</sup>H NMR (300 MHz, CDCl<sub>3</sub>):  $\delta$ =3.83 (s, 3H, MeO), 3.93 (s, 3H, MeO), 6.59 (d, <sup>4</sup>J<sub>H–H</sub>=2.7 Hz, 1H, Ar–H), 6.87 (d, <sup>4</sup>J<sub>H–H</sub>=2.7 Hz, 1H, Ar–H), 11.41 (s, 1H, OH). <sup>13</sup>C NMR (75 MHz, CDCl<sub>3</sub>):  $\delta$ =52.5 (MeO), 55.8 (MeO), 103.1 (C), 103.6 (CH), 109.3 (q, <sup>3</sup>J<sub>C–F</sub>=6.8 Hz, CH), 123.0 (q, <sup>1</sup>J<sub>C–F</sub>=271.5 Hz, CF<sub>3</sub>), 131.4 (q, <sup>2</sup>J<sub>C–F</sub>=31.5 Hz, C–CF<sub>3</sub>), 163.5 (C–OH), 165.1 (C–OMe), 169.7 (C=O). <sup>19</sup>F NMR (282.4 MHz, CDCl<sub>3</sub>):  $\delta$ =–58.9 (CF<sub>3</sub>). IR (ATR, cm<sup>–1</sup>):  $\tilde{\nu}$ =2957 (w), 2922 (w), 2853 (w), 1662 (m), 1614 (m), 1593 (m), 1440 (s), 1341 (m), 1312 (w), 1271 (m), 1136 (s), 1039 (m), 987 (m), 946 (m), 847 (m), 807 (m), 776 (w), 708 (m), 629 (s), 531 (s), 401 (s). GC–MS (EI, 70 eV): *m/z* (%): 250 (M<sup>+</sup>, 43), 219 (34), 218 (100), 190 (42), 175 (32), 171 (13), 147 (11). HRMS (EI, 70 eV): calcd for C<sub>10</sub>H<sub>9</sub>O<sub>4</sub>F<sub>3</sub> (M<sup>+</sup>): 250.04474; found: 250.044817.

**4.3.2. Isopropyl 2-hydroxy-4-methoxy-6-(trifluoromethyl)benzoate (3b).** Data have been previously reported.<sup>4b</sup> Starting with **1a** (0.184 g, 1.0 mmol), AlCl<sub>3</sub> (0.133 g, 1.0 mmol), **2b** (0.577 g, 2.0 mmol) in CH<sub>2</sub>Cl<sub>2</sub> (2.0 mL), **3b** was isolated as a yellowish solid (0.161 g, 58%); mp=44–48 °C. <sup>1</sup>H NMR (300 MHz, CDCl<sub>3</sub>):  $\delta$ =1.35 (d, <sup>3</sup>J<sub>H–H</sub>=6.0 Hz, 6H, CH<sub>3</sub>), 3.82 (s, 3H, MeO), 5.26 (m, 1H, CH), 6.57 (d, <sup>4</sup>J<sub>H–H</sub>=2.7 Hz, 1H, Ar–H), 6.72 (d, <sup>4</sup>J<sub>H–H</sub>=2.7 Hz, 1H, Ar–H), 11.68 (s, 1H, OH). <sup>13</sup>C NMR (75 MHz, CDCl<sub>3</sub>):  $\delta$ =21.3 (CH<sub>3</sub>), 21.3 (CH<sub>3</sub>), 55.7 (MeO), 70.4 (CH), 103.5 (C), 103.7 (CH), 109.2 (q, <sup>3</sup>J<sub>C–F</sub>=7.5 Hz, CH), 123.1 (q, <sup>1</sup>J<sub>C–F</sub>=274.5 Hz, CF<sub>3</sub>), 131.6 (q, <sup>2</sup>J<sub>C–F</sub>=33.8 Hz, C–CF<sub>3</sub>), 163.3

(C–OH), 165.2 (C–OMe), 168.8 (C=O). <sup>19</sup>F NMR (282.4 MHz, CDCl<sub>3</sub>):  $\delta$ =–57.7 (CF<sub>3</sub>).

IR (ATR, cm<sup>–1</sup>):  $\tilde{\nu}$ =3125 (w), 3098 (w), 3013 (w), 2987 (w), 2945 (w), 2852 (w), 1663 (m), 1618 (m), 1577 (w), 1492 (w), 1432 (w), 1365 (s), 1232 (s), 1134 (s), 1097 (s), 1042 (s), 987 (s), 912 (s), 844 (s), 712 (s), 620 (s), 529 (m), 481 (w), 429 (m). GC–MS (EI, 70 eV): *m/z* (%): 278 (M<sup>+</sup>, 15), 236 (17), 219 (31), 218 (100), 190 (28), 175 (15), 171 (8), 147 (6). HRMS (EI, 70 eV): calcd for C<sub>12</sub>H<sub>13</sub>O<sub>4</sub>F<sub>3</sub> (M<sup>+</sup>): 278.07604; found: 278.076053. Anal. Calcd for C<sub>12</sub>H<sub>13</sub>O<sub>4</sub>F<sub>3</sub> (278.22): C, 51.80; H, 4.71. Found: C, 52.12; H, 4.672.

**4.3.3. Isobutyl 2-hydroxy-4-methoxy-6-(trifluoromethyl)benzoate (3c).** Starting with **1a** (0.184 g, 1.0 mmol), AlCl<sub>3</sub> (0.133 g, 1.0 mmol), **2c** (0.605 g, 2.0 mmol) in CH<sub>2</sub>Cl<sub>2</sub> (2.0 mL), **3c** was isolated as a slight yellow solid (0.134 g, 46%); mp=40 °C. <sup>1</sup>H NMR (400 MHz, CDCl<sub>3</sub>):  $\delta$ =0.97 (d, <sup>3</sup>J<sub>H–H</sub>=6.8 Hz, 6H, CH<sub>3</sub>), 2.07 (m, 1H, CH), 3.82 (s, 3H, MeO), 4.12 (d, <sup>3</sup>J<sub>H–H</sub>=6.8 Hz, 2H, CH<sub>2</sub>), 6.59 (d, <sup>4</sup>J<sub>H–H</sub>=2.4 Hz, 1H, Ar–H), 6.86 (d, <sup>4</sup>J<sub>H–H</sub>=2.7 Hz, 1H, Ar–H), 11.64 (s, 1H, OH). <sup>13</sup>C NMR (100 MHz, CDCl<sub>3</sub>):  $\delta$ =19.1 (CH<sub>3</sub>), 19.1 (CH<sub>3</sub>), 27.5 (CH), 55.7 (MeO), 72.7 (CH<sub>2</sub>), 103.2 (C), 103.7 (CH), 109.2 (q, <sup>3</sup>J<sub>C–F</sub>=7.0 Hz, CH), 123.1 (q, <sup>1</sup>J<sub>C–F</sub>=271.0 Hz, CF<sub>3</sub>), 131.5 (q, <sup>2</sup>J<sub>C–F</sub>=32.0 Hz, C–CF<sub>3</sub>), 163.4 (C–OH), 165.3 (C–OMe), 169.6 (C=O). <sup>19</sup>F NMR (282.4 MHz, CDCl<sub>3</sub>):  $\delta$ =–58.3 (CF<sub>3</sub>). IR (ATR, cm<sup>–1</sup>):  $\tilde{\nu}$ =2967 (m), 2915 (w), 2877 (w), 2728 (w), 1648 (m), 1614 (m), 1594 (m), 1469 (m), 1427 (m), 1380 (m), 1331 (m), 1311 (m), 1272 (s), 1234 (m), 1211 (s), 1136 (s), 1041 (s), 989 (s), 856 (s), 628 (s), 540 (s), 445 (m), 387 (w). GC–MS (EI, 70 eV): *m/z* (%): 292 (M<sup>+</sup>, 18), 236 (18), 219 (37), 218 (100), 190 (21), 175 (9), 171 (10), 147 (6). HRMS (EI, 70 eV): calcd for C<sub>13</sub>H<sub>15</sub>O<sub>4</sub>F<sub>3</sub> (M<sup>+</sup>): 292.09170; found: 292.091940. Anal. Calcd for C<sub>13</sub>H<sub>15</sub>O<sub>4</sub>F<sub>3</sub> (292.25): C, 53.43; H, 5.17. Found: C, 53.40; H, 4.970.

**4.3.4. *n*-Butyl 2-hydroxy-4-methoxy-6-(trifluoromethyl)benzoate (3d).** Starting with **1a** (0.184 g, 1.0 mmol), AlCl<sub>3</sub> (0.133 g, 1.0 mmol), **2d** (0.605 g, 2.0 mmol) in CH<sub>2</sub>Cl<sub>2</sub> (2.0 mL), **3d** was isolated as a yellowish oil (0.154 g, 53%). <sup>1</sup>H NMR (400 MHz, CDCl<sub>3</sub>):  $\delta$ =0.95 (t, <sup>3</sup>J<sub>H–H</sub>=6.7 Hz, 3H, CH<sub>3</sub>), 1.42–1.46 (m, 2H, CH<sub>2</sub>), 1.70–1.77 (m, 2H, CH<sub>2</sub>), 3.82 (s, 3H, MeO), 4.33 (t, <sup>3</sup>J<sub>H–H</sub>=6.8 Hz, 2H, OCH<sub>2</sub>), 6.58 (d, <sup>4</sup>J<sub>H–H</sub>=2.8 Hz, 1H, Ar–H), 6.86 (d, <sup>4</sup>J<sub>H–H</sub>=2.8 Hz, 1H, Ar–H), 11.61 (s, 1H, OH). <sup>13</sup>C NMR (100 MHz, CDCl<sub>3</sub>):  $\delta$ =13.5 (CH<sub>3</sub>), 18.9 (CH<sub>2</sub>), 30.0 (CH<sub>2</sub>), 55.6 (MeO), 66.1 (OCH<sub>2</sub>), 103.2 (C), 103.5 (CH), 109.1 (q, <sup>3</sup>J<sub>C–F</sub>=7.0 Hz, CH), 123.0 (q, <sup>1</sup>J<sub>C–F</sub>=271.0 Hz, CF<sub>3</sub>), 131.6 (q, <sup>2</sup>J<sub>C–F</sub>=32.0 Hz, C–CF<sub>3</sub>), 163.3 (C–OH), 165.1 (C–OMe), 169.4 (C=O). <sup>19</sup>F NMR (282.4 MHz, CDCl<sub>3</sub>):  $\delta$ =–58.3 (CF<sub>3</sub>). IR (ATR, cm<sup>–1</sup>):  $\tilde{\nu}$ =2964 (m), 2938 (w), 2874 (w), 1652 (m), 1616 (m), 1592 (m), 1442 (m), 1425 (m), 1386 (m), 1334 (m), 1310 (m), 1276 (s), 1235 (m), 1206 (s), 1136 (s), 1040 (s), 988 (s), 863 (s), 715 (s), 627 (s), 534 (s), 445 (m), 380 (w). GC–MS (EI, 70 eV): *m/z* (%): 292 (M<sup>+</sup>, 19), 219 (26), 218 (100), 190 (22). HRMS (EI, 70 eV): calcd for C<sub>13</sub>H<sub>15</sub>O<sub>4</sub>F<sub>3</sub> (M<sup>+</sup>): 292.09170; found: 292.091638. Anal. Calcd for C<sub>13</sub>H<sub>15</sub>F<sub>3</sub>O<sub>4</sub> (292.25): C, 53.43; H, 5.17. Found: C, 53.34; H, 5.231.

**4.3.5. Isopentyl 2-hydroxy-4-methoxy-6-(trifluoromethyl)benzoate (3e).** Starting with **1a** (0.184 g, 1.0 mmol), AlCl<sub>3</sub> (0.133 g, 1.0 mmol), **2e** (0.633 g, 2.0 mmol) in CH<sub>2</sub>Cl<sub>2</sub> (2.0 mL), **3e** was isolated as a slight yellow oil (0.140 g, 46%). <sup>1</sup>H NMR (300 MHz, CDCl<sub>3</sub>):  $\delta$ =0.97 (d, <sup>3</sup>J<sub>H–H</sub>=6.8 Hz, 6H, CH<sub>3</sub>), 1.60–1.80 (m, 3H, CH and CH<sub>2</sub>), 3.86 (s, 3H, MeO), 4.35 (t, <sup>3</sup>J<sub>H–H</sub>=6.9 Hz, 2H, OCH<sub>2</sub>), 6.58 (d, <sup>4</sup>J<sub>H–H</sub>=2.8 Hz, 1H, Ar–H), 6.86 (d, <sup>4</sup>J<sub>H–H</sub>=2.8 Hz, 1H, Ar–H), 11.61 (s, 1H, OH). <sup>13</sup>C NMR (75 MHz, CDCl<sub>3</sub>):  $\delta$ =22.3 (CH<sub>3</sub>), 22.3 (CH<sub>3</sub>), 24.7 (CH), 36.7 (CH<sub>2</sub>), 55.7 (MeO), 64.9 (OCH<sub>2</sub>), 103.3 (C), 103.6 (CH), 109.2 (q, <sup>3</sup>J<sub>C–F</sub>=7.5 Hz, CH), 123.1 (q, <sup>1</sup>J<sub>C–F</sub>=271.5 Hz, CF<sub>3</sub>), 131.7 (q, <sup>2</sup>J<sub>C–F</sub>=31.5 Hz, C–CF<sub>3</sub>), 163.4 (C–OH), 165.2 (C–OMe), 169.5 (C=O). <sup>19</sup>F NMR (282.4 MHz, CDCl<sub>3</sub>):  $\delta$ =–58.3 (CF<sub>3</sub>). IR (ATR, cm<sup>–1</sup>):  $\tilde{\nu}$ =2960 (m), 2872 (w), 1660 (w), 1619 (m),

1446 (w), 1275 (m), 1233 (s), 1137 (s), 1043 (s), 990 (s), 943 (m), 715 (s), 626 (m), 531 (m), 469 (m), 401 (m). GC–MS (EI, 70 eV):  $m/z$  (%): 306 ( $M^+$ , 14), 237 (8), 236 (16), 219 (33), 218 (100), 190 (16), 43 (10). HRMS (EI, 70 eV): calcd for  $C_{14}H_{17}O_4F_3$  ( $M^+$ ): 306.10735; found: 306.107777. Anal. Calcd for  $C_{14}H_{17}O_4F_3$  (306.28): C, 54.90; H, 5.59. Found: C, 54.87; H, 5.605.

**4.3.6. *n*-Octyl 2-hydroxy-4-methoxy-6-(trifluoromethyl)benzoate (3f).** Starting with **1a** (0.184 g, 1.0 mmol),  $AlCl_3$  (0.133 g, 1.0 mmol), **2f** (0.717 g, 2.0 mmol) in  $CH_2Cl_2$  (2.0 mL), **3f** was isolated as a slight yellow solid (0.177 g, 51%); mp=37–39 °C.  $^1H$  NMR (400 MHz,  $CDCl_3$ ):  $\delta$ =0.88 (t,  $^3J_{H-H}$ =7.0 Hz, 3H,  $CH_3$ ), 1.18–1.39 (m, 10H,  $CH_2$ ), 1.72–1.76 (m, 2H,  $CH_2$ ), 3.82 (s, 3H, MeO), 4.31 (t,  $^3J_{H-H}$ =6.8 Hz, 2H,  $OCH_2$ ), 6.58 (d,  $^4J_{H-H}$ =2.4 Hz, 1H, Ar–H), 6.86 (d,  $^4J_{H-H}$ =2.4 Hz, 1H, Ar–H), 11.61 (s, 1H, OH).  $^{13}C$  NMR (100 MHz,  $CDCl_3$ ):  $\delta$ =13.8 ( $CH_3$ ), 22.4 ( $CH_2$ ), 25.5 ( $CH_2$ ), 27.9 ( $CH_2$ ), 28.9 ( $CH_2$ ), 31.5 ( $CH_2$ ), 55.5 (MeO), 66.3 ( $OCH_2$ ), 103.1 (C), 103.4 (CH), 109.0 (q,  $^3J_{C-F}$ =7.0 Hz, CH), 122.9 (q,  $^1J_{C-F}$ =271.0 Hz,  $CF_3$ ), 131.5 (q,  $^2J_{C-F}$ =32.0 Hz, C– $CF_3$ ), 163.2 (C–OH), 165.1 (C–OMe), 169.3 (C=O).  $^{19}F$  NMR (282.4 MHz,  $CDCl_3$ ):  $\delta$ =–58.3 ( $CF_3$ ). IR (ATR,  $cm^{-1}$ ):  $\tilde{\nu}$ =3087 (w), 2963 (w), 2925 (w), 2856 (w), 1656 (m), 1614 (m), 1448 (m), 1429 (m), 1388 (w), 1333 (m), 1312 (w), 1277 (m), 1235 (m), 1213 (m), 1144 (s), 1040 (s), 987 (s), 940 (s), 867 (m), 808 (s), 713 (s), 629 (m), 538 (m), 495 (m), 397 (m). GC–MS (EI, 70 eV):  $m/z$  (%): 348 ( $M^+$ , 13), 236 (25), 219 (27), 218 (100), 190 (10). HRMS (EI, 70 eV): calcd for  $C_{17}H_{23}O_4F_3$  ( $M^+$ ): 348.15430; found: 348.154113. Anal. Calcd for  $C_{17}H_{23}O_4F_3$  (348.36): C, 58.61; H, 6.65. Found: C, 58.62; H, 6.669.

**4.3.7. Methyl 2-hydroxy-4-methoxy-3-methyl-6-(trifluoromethyl)benzoate (3g).** Data have been previously reported.<sup>4b</sup> Starting with **1a** (0.184 g, 1.0 mmol),  $AlCl_3$  (0.133 g, 1.0 mmol), **2g** (0.549 g, 2.0 mmol) in  $CH_2Cl_2$  (2.0 mL), **3g** was isolated as a slight yellow solid (0.132 g, 50%); mp=67 °C.  $^1H$  NMR (300 MHz,  $CDCl_3$ ):  $\delta$ =2.11 (s, 3H,  $CH_3$ ), 3.89 (s, 3H, MeO), 3.93 (s, 3H, MeO), 6.84 (s, 1H, CH), 11.25 (s, 1H, OH).  $^{13}C$  NMR (75 MHz,  $CDCl_3$ ):  $\delta$ =8.3 ( $CH_3$ ), 52.6 (MeO), 55.8 (MeO), 102.5 (q,  $^3J_{C-F}$ =6.75 Hz, CH), 104.0 (C), 117.7 (C), 123.5 (q,  $^1J_{C-F}$ =271.5 Hz,  $CF_3$ ), 128.9 (q,  $^2J_{C-F}$ =31.5 Hz, C– $CF_3$ ), 160.7 (C–OH), 161.3 (C–OMe), 170.1 (C=O).  $^{19}F$  NMR (282.4 MHz,  $CDCl_3$ ):  $\delta$ =–58.2 ( $CF_3$ ). IR (ATR,  $cm^{-1}$ ):  $\tilde{\nu}$ =2957 (w), 2929 (w), 2864 (w), 1656 (s), 1606 (s), 1586 (m), 1438 (m), 1401 (m), 1337 (m), 1315 (m), 1286 (s), 1247 (s), 1204 (s), 1122 (s), 998 (s), 927 (s), 841 (s), 805 (s), 712 (m), 677 (m), 545 (m), 418 (m), 396 (w). GC–MS (EI, 70 eV):  $m/z$  (%): 264 ( $M^+$ , 77), 233 (43), 232 (100), 231 (13), 214 (15), 213 (9), 212 (57), 204 (66), 203 (17), 202 (26), 185 (15), 182 (11). HRMS (EI, 70 eV): calcd for  $C_{11}H_{21}O_4F_3$  ( $M^+$ ): 264.06039; found: 264.060573. Anal. Calcd for  $C_{11}H_{21}O_4F_3$  (264.20): C, 50.01; H, 4.20. Found: C, 50.41; H, 4.588.

**4.3.8. Methyl 2-hydroxy-4-methoxy-3-ethyl-6-(trifluoromethyl)benzoate (3h).** Starting with **1a** (0.184 g, 1.0 mmol),  $AlCl_3$  (0.133 g, 1.0 mmol), **2h** (0.577 g, 2.0 mmol) in  $CH_2Cl_2$  (2.0 mL), **3h** was isolated as a yellowish solid (0.161 g, 58%); mp=46 °C.  $^1H$  NMR (300 MHz,  $CDCl_3$ ):  $\delta$ =1.08 (t,  $^3J_{H-H}$ =7.8 Hz, 3H,  $CH_3$ ), 2.68 (q,  $^3J_{H-H}$ =7.2 Hz, 2H,  $CH_2$ ), 3.88 (s, 3H, MeO), 3.93 (s, 3H, MeO), 6.85 (s, 1H, CH), 11.18 (s, 1H, OH).  $^{13}C$  NMR (75 MHz,  $CDCl_3$ ):  $\delta$ =12.8 ( $CH_3$ ), 16.4 ( $CH_2$ ), 52.5 (MeO), 55.7 (MeO), 102.7 (q,  $^3J_{C-F}$ =7.5 Hz, CH), 104.2 (C), 118.0 (C), 123.6 (q,  $^1J_{C-F}$ =271.5 Hz,  $CF_3$ ), 129.0 (q,  $^2J_{C-F}$ =31.5 Hz, C– $CF_3$ ), 160.5 (C–OH), 161.1 (C–OMe), 170.2 (C=O).  $^{19}F$  NMR (282.4 MHz,  $CDCl_3$ ):  $\delta$ =–58.2 ( $CF_3$ ). IR (ATR,  $cm^{-1}$ ):  $\tilde{\nu}$ =3026 (w), 2980 (w), 2957 (w), 2877 (w), 2857 (w), 1672 (s), 1599 (s), 1504 (s), 1438 (s), 1402 (m), 1316 (s), 1244 (s), 1204 (m), 1179 (s), 1120 (s), 1003 (w), 968 (m), 946 (m), 917 (m), 845 (s), 804 (m), 764 (m), 635 (m), 610 (m), 543 (m), 396 (s). GC–MS (EI, 70 eV):  $m/z$  (%): 278 ( $M^+$ , 72), 247 (37), 246 (100), 231 (36), 226 (44), 218 (72), 208 (16), 203 (12), 200 (15), 181 (16), 175 (20). HRMS (EI, 70 eV): calcd

for  $C_{12}H_{13}O_4F_3$  ( $M^+$ ): 278.07604; found: 278.076396. Anal. Calcd for  $C_{12}H_{13}O_4F_3$  (278.22): C, 51.80; H, 4.71. Found: C, 51.89; H, 4.723.

**4.3.9. Methyl 2-hydroxy-4-methoxy-3-nonyl-6-(trifluoromethyl)benzoate (3i).** Starting with **1a** (0.184 g, 1.0 mmol),  $AlCl_3$  (0.133 g, 1.0 mmol), **2i** (0.733 g, 2.0 mmol) in  $CH_2Cl_2$  (2.0 mL), **3i** was isolated as a slight yellow solid (0.196 g, 52%); mp=47 °C.  $^1H$  NMR (400 MHz,  $CDCl_3$ ):  $\delta$ =0.87 (t,  $^3J_{H-H}$ =8.0 Hz, 3H,  $CH_3$ ), 1.25–1.49 (m, 14H,  $CH_2$ ), 2.66 (t,  $^3J_{H-H}$ =8.0 Hz, 3H,  $CH_2$ ), 3.88 (s, 3H, MeO), 3.93 (s, 3H, MeO), 6.85 (s, 1H, CH), 11.18 (s, 1H, OH).  $^{13}C$  NMR (75 MHz,  $CDCl_3$ ):  $\delta$ =12.6 ( $CH_3$ ), 21.2, 21.2, 21.6, 21.6, 26.0, 27.2, 27.8, 27.8, 30.5, 30.8, 30.8, 31.6 ( $CH_2$ ), 50.4 (MeO), 55.3 (MeO), 101.4 (q,  $^3J_{C-F}$ =6.9 Hz, CH), 102.9 (C), 121.3 (C), 122.3 (q,  $^1J_{C-F}$ =271.0 Hz,  $CF_3$ ), 127.6 (q,  $^2J_{C-F}$ =31.0 Hz, C– $CF_3$ ), 159.4 (C–OH), 159.7 (C–OMe), 168.9 (C=O).  $^{19}F$  NMR (282.4 MHz,  $CDCl_3$ ):  $\delta$ =–58.3 ( $CF_3$ ). IR (ATR,  $cm^{-1}$ ):  $\tilde{\nu}$ =2955 (m), 2914 (s), 2850 (m), 1656 (m), 1583 (w), 1441 (s), 1404 (m), 1312 (s), 1250 (s), 1207 (s), 1127 (s), 1079 (m), 1003 (s), 932 (s), 864 (s), 811 (m), 716 (s), 692 (m), 572 (m), 487 (w), 425 (m), 406 (m). GC–MS (EI, 70 eV):  $m/z$  (%): 376 ( $M^+$ , 32), 345 (17), 344 (13), 327 (16), 314 (14), 313 (79), 245 (18), 233 (13), 232 (100), 231 (87), 212 (15), 204 (21), 201 (10), 181 (20). HRMS (EI, 70 eV): calcd for  $C_{19}H_{27}O_4F_3$  ( $M^+$ ): 376.18560; found: 376.185024. Anal. Calcd for  $C_{19}H_{27}O_4F_3$  (376.41): C, 60.63; H, 7.23. Found: C, 60.87; H, 7.290.

**4.3.10. Methyl 2-hydroxy-4-methoxy-3-tetradecyl-6-(trifluoromethyl)benzoate (3j).** Starting with **1a** (0.184 g, 1.0 mmol),  $AlCl_3$  (0.133 g, 1.0 mmol), **2j** (0.914 g, 2.0 mmol) in  $CH_2Cl_2$  (2.0 mL), **3j** was isolated as a slight yellow solid (0.209 g, 47%); mp=67 °C.  $^1H$  NMR (300 MHz,  $CDCl_3$ ):  $\delta$ =0.89 (t,  $^3J_{H-H}$ =7.6 Hz, 3H,  $CH_3$ ), 1.17–1.48 (m, 24H,  $CH_2$ ), 2.63 (t,  $^3J_{H-H}$ =7.6 Hz, 2H,  $CH_2$ ), 3.89 (s, 3H, MeO), 3.93 (s, 3H, MeO), 6.84 (s, 1H, CH), 11.18 (s, 1H, OH).  $^{13}C$  NMR (75 MHz,  $CDCl_3$ ):  $\delta$ =14.1 ( $CH_3$ ), 22.7, 23.0, 28.3, 29.4, 29.5, 29.5, 29.7, 29.7, 29.7, 29.7, 29.8, 31.9, 52.5 (MeO), 55.7 (MeO), 102.7 (q,  $^3J_{C-F}$ =7.5 Hz, CH), 104.2 (C), 122.5 (CH), 123.5 (q,  $^1J_{C-F}$ =270.8 Hz,  $CF_3$ ), 129.0 (q,  $^2J_{C-F}$ =31.5 Hz, C– $CF_3$ ), 160.7 (C–OH), 161.3 (C–OMe), 170.2 (C=O).  $^{19}F$  NMR (282.4 MHz,  $CDCl_3$ ):  $\delta$ =–58.2 ( $CF_3$ ). IR (ATR,  $cm^{-1}$ ):  $\tilde{\nu}$ =2953 (s), 2915 (s), 2848 (s), 1657 (s), 1612 (w), 1583 (w), 1464 (m), 1442 (m), 1405 (m), 1323 (m), 1251 (s), 1207 (s), 1127 (m), 1079 (m), 999 (m), 933 (m), 860 (m), 779 (w), 717 (s), 692 (m), 545 (m), 476 (w), 426 (w), 401 (w). GC–MS (EI, 70 eV):  $m/z$  (%): 446 ( $M^+$ , 24), 415 (12), 414 (13), 397 (14), 384 (15), 383 (66), 245 (17), 233 (18), 232 (100), 231 (87), 212 (13), 204 (16), 181 (14). HRMS (EI, 70 eV): calcd for  $C_{24}H_{37}O_4F_3$  ( $M^+$ ): 446.26385; found: 446.263600.

#### 4.4. X-ray crystal structure analysis of 5

The structure analysis was carried out by using a Bruker Kappa APEX II duo diffractometer, using graphite-monochromated  $MoK\alpha$  radiation. The structure was solved by direct methods and refined by full-matrix least-squares procedures on  $F^2$  with the SHELXTL software package.<sup>25</sup> Crystal data:  $C_{15}H_{12}AlF_9O_9$ ,  $M=534.23$ , monoclinic, space group  $P2_1/n$ ,  $a=7.0281(1)$ ,  $b=19.5037(3)$ ,  $c=15.0327(2)$  Å,  $\beta=98.170(1)^\circ$ ,  $V=2039.68(5)$  Å<sup>3</sup>,  $T=150(2)$  K,  $Z=4$ , 17,010 reflections measured, 4686 independent reflections ( $R_{int}=0.0234$ ), final  $R$  values ( $I>2\sigma(I)$ ):  $R_1=0.0343$ ,  $wR_2=0.0822$ , final  $R$  values (all data):  $R_1=0.0464$ ,  $wR_2=0.0906$ , 310 refined parameters.

CCDC 896100 contains the supplementary crystallographic data for this paper. These data can be obtained free of charge from The Cambridge Crystallographic Data Centre via [www.ccdc.cam.ac.uk/data\\_request/cif](http://www.ccdc.cam.ac.uk/data_request/cif).

#### 4.5. Coupled in situ ATR-FTIR/UV–vis spectroscopy

The reaction was carried out in a homemade reaction cell<sup>5</sup> under inert atmosphere. The reaction cell was flushed with argon before

reaction and during dosing when the cell was open. The cooling has been performed by a Julabo cryostat. 4,4-Dimethoxy-1,1,1-trifluorobut-3-en-2-one **1a** (736 mg, 4.0 mmol) has been dissolved in CH<sub>2</sub>Cl<sub>2</sub> (8.0 mL) at room temperature. The cooling started and AlCl<sub>3</sub> was added when a temperature of 0 °C (533 mg, 4.0 mmol) was reached. The cooling was continued and 1,3-bis(silyloxy)-1,3-butadienes **2** (2.080 g, 8.0 mmol) was added at –60 °C. Afterward the mixture was warmed up to 0 °C during a 4 h period with stirring. Finally the reaction was quenched by adding hydrochloric acid (60.0 mL, 10%) to the reaction mixture. The in situ ATR-FTIR spectra were measured with a fiber optical diamond ATR probe (infrared fiber sensors, Aachen, Germany), which was connected to a Nicolet Avatar 370 (Thermo Electron) FTIR spectrometer. All spectra were recorded with 128 scans at 4 cm<sup>-1</sup> resolution. The ex situ ATR-FTIR spectra were measured with a Bruker Alpha spectrometer equipped with a Platinum ATR single reflection diamond ATR. The spectra were recorded with 32 scans at 4 cm<sup>-1</sup> resolution at room temperature.

The UV–vis spectra were sampled with an AvaSpec 2048 fiber optical spectrometer (Avantes B.V., Eerbeek, Netherlands) equipped with an AvaLight-DHS light source and an FCR-7xx200-2-45 reflection probe for the solid samples and an FDP-UV-micro-1 transmission probe for the liquid samples. All spectra of the solid samples were recorded with 30 accumulations and an integration time of 23 ms, and all spectra of liquid samples were recorded with 50 accumulations and an integration time of 10 ms.

#### 4.6. Quantum chemical studies

The vertical excitation spectra of the Al-complex, Ti-complex,<sup>5</sup> and butenone **1a**, have been investigated using time-dependent density functional theory employing the B3LYP functional (m3 grid) with a def2-TVZP basis set as implemented in Turbomole.<sup>19</sup> Starting from the available crystal structures (Ti-complex, Al-complex) ground state optimizations have been performed in gas phase. Vertical excitation spectra are calculated for the Ti-complex (30 roots), Al-complex (20 roots), and **1a** (20 roots), taking into account the solvent (CH<sub>2</sub>Cl<sub>2</sub>) by means of the COSMO conductor-like screening model.<sup>26</sup>

#### 4.7. General procedure for the synthesis of **3a** and **3b** by utilization of TiO<sub>2</sub> or Al<sub>2</sub>O<sub>3</sub> as mediating acid

TiO<sub>2</sub> and Al<sub>2</sub>O<sub>3</sub> were activated under vacuum by repeated heating for 2–3 h and stored under Argon before use (The reaction with non-activated TiO<sub>2</sub> and Al<sub>2</sub>O<sub>3</sub> did not proceed.) TiO<sub>2</sub> or Al<sub>2</sub>O<sub>3</sub> (1.0 mmol) was added under argon to a vigorously stirred solution of **1a** (1.0 mmol) and 1,3-bis(silyloxy)-1,3-butadienes **2** (2.0 mmol) in CH<sub>2</sub>Cl<sub>2</sub> (1.0 mL) at 0 °C (ice bath). The reaction mixture was allowed to warm to room temperature for 8 h period with stirring. CH<sub>2</sub>Cl<sub>2</sub> (15.0 mL) was added and the mixture was filtered. To the filtrate was added HCl (10%, 15.0 mL) and the organic and aqueous layers were separated. The latter was extracted with CH<sub>2</sub>Cl<sub>2</sub> (3×15.0 mL). The combined organic layers were dried (Na<sub>2</sub>SO<sub>4</sub>), filtered, and the filtrate was concentrated in vacuo. The residue was purified by flash chromatography using *n*-heptane and ethyl acetate.

#### 4.8. Adsorption experiments

The substrates **1a** and **2a** were separately adsorbed on Al<sub>2</sub>O<sub>3</sub> or TiO<sub>2</sub> by stirring a suspension of Al<sub>2</sub>O<sub>3</sub> or TiO<sub>2</sub> for 1 h at room temperature. The volume of CH<sub>2</sub>Cl<sub>2</sub> was 2.0 mL and the concentration of the substrate 0.5 mol L<sup>-1</sup>. The used amounts of the solids were 0.166 g of Al<sub>2</sub>O<sub>3</sub> and 0.120 g of TiO<sub>2</sub>. Afterward the mixture was filtrated over Whatman Qualitative 5 filtration papers, washed with three portions of 5 mL each CH<sub>2</sub>Cl<sub>2</sub> and dried over night on air.

The adsorbed species were pressed to self-supporting wafers for analysis by FTIR transmission spectroscopy. Samples in powder-form were used for the analysis by UV–vis-DRS spectroscopy. The self-supporting wafers were made by pressing 50 mg material with 10 t to a disc with a diameter of 20 mm. The analysis was done with a Bruker Tensor 27 spectrometer. The spectra were recorded with 32 scans at 2 cm<sup>-1</sup> resolution.

#### Acknowledgements

S.R. would like to acknowledge gratefully the University of Rostock (scholarship of the interdisciplinary faculty of the University of Rostock/Dept. LLM) and the State of Mecklenburg-Vorpommern for financial support. Dr. L.R.K. would like to thank gratefully the Leibniz Society for financial support.

#### Supplementary data

Additional information concerning the molecular structure, Raman- and ATR-FTIR spectra of the Al tris-chelate complex **5** as well as calculation of the excitation spectra. <sup>1</sup>H NMR and <sup>13</sup>C NMR spectra of **3a–3j**. Supplementary data associated with this article can be found, in the online version, at <http://dx.doi.org/10.1016/j.tet.2013.01.097>.

#### References and notes

- (a) Tietze, L. F.; Beifuss, U. *Angew. Chem.* **1993**, *105*, 137–170; *Angew. Chem., Int. Ed. Engl.* **1993**, *32*, 131–163; (b) Brownbridge, P. *Synthesis* **1983**, 85–104; (c) Jørgensen, K. A. *Angew. Chem.* **2000**, *112*, 3702–3733; *Angew. Chem. Int. Ed.* **2000**, *39*, 3558–3588; (d) Danishefsky, S. J.; Bilodeau, M. T. *Angew. Chem.* **1996**, *108*, 1482–1522; *Angew. Chem. Int. Ed.* **1996**, *35*, 1380–1419.
- (a) Feist, H.; Langer, P. *Synthesis* **2007**, *3*, 1–10; (b) Langer, P. *Synthesis* **2002**, 441–459; (c) Langer, P. *Synlett* **2006**, 3369–3381.
- (a) Erfle, S.; Reimann, S.; Bunescu, A.; Abilov, Z. A.; Spannenberg, A.; Langer, P. *Helv. Chim. Acta* **2012**, *95*, 1037–1047; (b) Büttner, S.; Kelzhanova, N. K.; Abilov, Z. A.; Villinger, A.; Langer, P. *Tetrahedron* **2012**, *10*, 3654–3688; (c) Iaroshenko, V. O.; Bunescu, A.; Supe, L.; Milyutina, M.; Spannenberg, A.; Langer, P. *Org. Biomol. Chem.* **2011**, *9*, 7554–7558; (d) Iaroshenko, V. O.; Bunescu, A.; Domke, L.; Spannenberg, A.; Sevenard, D.; Villinger, A.; Sosnovskikh, V. Y.; Langer, P. *J. Fluorine Chem.* **2011**, *132*, 441–449; (e) Iaroshenko, V. O.; Bunescu, A.; Spannenberg, A.; Langer, P. *Chem.—Eur. J.* **2011**, *17*, 7188–7192.
- (a) Reimann, S.; Bunescu, A.; Litschko, R.; Erfle, S.; Domke, L.; Bendrath, F.; Abilov, Z. A.; Spannenberg, A.; Villinger, A.; Langer, P. *J. Fluorine Chem.* **2012**, *139*, 28–45; (b) Bunescu, A.; Reimann, S.; Lubbe, M.; Spannenberg, A.; Langer, P. *J. Org. Chem.* **2009**, *74*, 5002–5010; (c) Kapapetyan, V.; Mkrtchyan, S.; Ghazaryan, G.; Villinger, A.; Fischer, C.; Langer, P. *Tetrahedron* **2009**, *65*, 9271–9279.
- Knöpke, L. R.; Reimann, S.; Spannenberg, A.; Langer, P.; Brückner, A.; Bentrup, U. *ChemCatChem* **2011**, *3*, 1459–1468.
- (a) Kobayashi, S.; Busujima, T.; Nagayama, S. *Chem.—Eur. J.* **2000**, *6*, 3491–3494; (b) Olah, G. A.; Kobayashi, S.; Tashiro, M. *J. Am. Chem. Soc.* **1972**, *94*, 7448–7461.
- For example: (a) Langer, P.; Bose, G. *Angew. Chem. Int. Ed.* **2003**, *42*, 4033–4036; (b) Ullah, E.; Appel, B.; Fischer, C.; Langer, P. *Tetrahedron* **2006**, *62*, 9694–9700; (c) Ahmed, Z.; Fischer, C.; Spannenberg, A.; Langer, P. *Tetrahedron* **2006**, *62*, 4800–4806; (d) Kobayashi, S. *Eur. J. Org. Chem.* **1999**, 15–27; (e) Momiyama, N.; Yamamoto, H. *Angew. Chem.* **2002**, *114*, 3112–3114.
- (a) Yamamoto, H. *Lewis Acids in Organic Synthesis*; Wiley-VCH: Weinheim, Germany, 2000; Vol. 1; (b) Yamamoto, H. *Lewis Acid Reagents*; Oxford University Press: Oxford, 1999; (c) Schinzer, D. *Selectivities in Lewis Acid Promoted Reactions*; Kluwer: Dordrecht, The Netherlands, 1989.
- (a) Belova, N. V.; Dalhus, B.; Girichev, G. V.; Giricheva, N. I.; Haaland, A.; Kuzmima, N. P.; Zhukova, T. A. *Struct. Chem.* **2011**, *22*, 393–399; (b) Shirodker, M.; Borker, V.; Nather, C.; Bensch, W.; Rane, K. S. *Indian J. Chem., Sect. A* **2010**, *49*, 1607–1611; (c) Tayyari, S. F.; Raissi, H.; Ahmadabadi, Z. *Spectrochim. Acta, Part A* **2002**, *58*, 2669–2682; (d) Diaz-Acosta, I.; Baker, J.; Cordes, W.; Pulay, P. *J. Phys. Chem. A* **2000**, *105*, 238–244; (e) Ferraro, J. R. *Low-Frequency Vibrations of Inorganic and Coordination Compounds*; Plenum: New York, NY, 1971; p 94.
- (a) Chan, T.-H.; Brownbridge, P. *J. Am. Chem. Soc.* **1980**, *102*, 3534–3538; (b) Molander, G. A.; Cameron, K. O. *J. Am. Chem. Soc.* **1993**, *115*, 830–846; (c) Nguyen, V. T. H.; Bellur, E.; Appel, B.; Langer, P. *Synthesis* **2006**, 2865–2872.
- Pasynkiewicz, S.; Starowiejski, K. B.; Peregodov, A. S.; Kravtsov, D. N. *J. Organomet. Chem.* **1977**, *132*, 191–201.
- McIntyre, J. F.; Foley, R. T.; Brown, B. F. *Inorg. Chem.* **1982**, *21*, 1167–1172.
- Holm, R. H.; Cotton, F. A. *J. Am. Chem. Soc.* **1958**, *80*, 5658–5663.
- Nakamoto, K.; McCarthy, P. J.; Ruby, A.; Martell, A. E. *J. Am. Chem. Soc.* **1961**, *83*, 1066–1069.
- Nakamoto, K.; McCarthy, P. J.; Martell, A. E. *J. Am. Chem. Soc.* **1961**, *83*, 1272–1276.

16. Masui, H. *Coord. Chem. Rev.* **2001**, 219–221, 957–992.
17. TURBOMOLE V6.3 2011, A development of University of Karlsruhe and Forschungszentrum Karlsruhe GmbH, 1989–2007, TURBOMOLE GmbH, since 2007. Available from: <http://www.turbomole.com>.
18. Onishi, T.; Shimanouchi, T. *Spectrochim. Acta* **1964**, 20, 325–338.
19. Mann, G.; Haaland, A.; Weidlein, J. Z. *Anorg. Allg. Chem.* **1973**, 398, 231–240.
20. Derouault, J.; Forel, M. *Inorg. Chem.* **1977**, 16, 3207–3213.
21. Altwood, J. L.; Jones, C.; Raston, C. L.; Robinson, K. D. *Main Group Chem.* **1996**, 1, 345–347.
22. (a) Clark, J. H.; Rhodes, C. N. *Clean Synthesis Using Porous Inorganic Solid Catalysts and Supported Reagents*; The Royal Society of Chemistry: Cambridge, UK, 2000; (b) Thomas, J. M.; Thomas, W. J. *Principles and Practice of Heterogeneous Catalysis*; Wiley-VCH: Weinheim, Germany, 1996; Chapter 8; (c) Basu, B.; Das, P.; Das, S. *Curr. Org. Chem.* **2008**, 12, 141–158.
23. Egerton, T. A.; Everall, N. J.; Mattinson, J. A.; Kessell, L. M.; Tooley, I. R. *J. Photochem. Photobiol. A* **2008**, 193, 10–17.
24. (a) Posner, G. H. *Angew. Chem.* **1978**, 90, 527–536; *Angew. Chem., Int. Ed. Engl.* **1978**, 17, 487–496; (b) Ranu, B. C.; Saha, M.; Bhar, S. *J. Chem. Soc., Perkin Trans. 1* **1994**, 2197–2199.
25. Sheldrick, G. M. *Acta Crystallogr.* **2008**, A64, 112–122.
26. Schäfer, A.; Klamt, A.; Sattel, D.; Lohrenz, J.; Eckert, F. *Phys. Chem. Chem. Phys.* **2000**, 2, 2187–2193.